2024 International Symposium on Electromagnetic Compatibility – EMC Europe | 979-8-3503-0735-1/24/$31.00 ©2024 IEEE | DOI: 10.1109/EMCEurope59828.2024.10722433

Direct Lightning of a Compact Overhead Distribution Line with Covered Conductors and Periodic Grounding

Erika Stracqualursi[#], Gianfranco Di Lorenzo[#], J. Brandão Faria[*], Rodolfo Araneo[#]
[#]Electrical Engineering Division of DIAEE, University of Rome "Sapienza", Italy
[*]Instituto de Telecomunicacoes, Instituto Superior Tecnico – Universidade de Lisboa, Portugal
{erika.stracqualursi, gianfranco.dilorenzo, rodolfo.araneo}@uniroma1.it, brandao.faria@tecnico.ulisboa.pt

***Abstract* — Covered conductors are adopted for medium and high voltage overhead lines to limit the line right-of-way and the occurrence of faults to ground caused by external agents. The insulating layer of the phase aerial cables allows to diminish maintenance pruning in rural or remote areas and increase the resilience of these compact lines with respect to extreme weather events. This paper assesses the modeling of the line and the analysis of the results related to direct lightning of the messenger wire, i.e., the upper bare conductor installed for mechanical support. Indeed, in case of direct lightning, the messenger wire may act as an unintentional shield wire. Travelling voltages due to direct lightning of a compact distribution line are calculated, while investigating also the insulation withstand capability.**

***Keywords* — chain matrix analysis, compact overhead line, covered conductors, direct lightning, lightning transients, periodical grounding.**

I. Introduction

Climate change and extreme weather events have raised the interest for alternative, more robust technical solutions for the installation of overhead distribution and transmission lines.

Lines with covered conductors represent a technology adopted in several countries (e.g., Thailand, Vietnam, Myanmar, US) at different voltage levels. Covered conductors typically consist of stranded conductors. Depending on the voltage rating, these are coated with up to three extruded layers. This technology is often chosen for its robustness. The phase conductor additional insulation prevents faults to ground in case of direct contact with vegetation. Additionally, it allows reduced clearance distances and right-of-way, enabling installation also within urban areas. The technology allows to improve the distribution quality indexes, i.e., the system average interruption frequency index and the system average interruption duration index, defined in the IEEE Std. 1366 [1].

As a drawback, unlike typical bare-wire systems with self-restoring insulation, the formation of pinholes may permanently impair the performance of the external insulating layer of aerial cables. Several experimental studies have been performed on aerial cables with punctured insulation [2], highlighting a decreased insulation impulse withstand voltage [3].

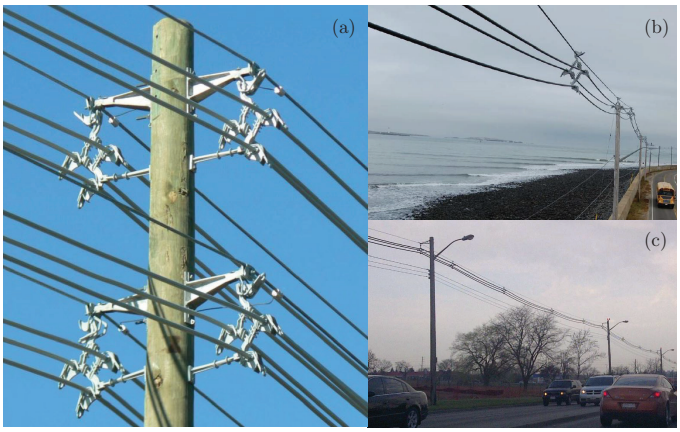

Fig. 1. (a) Four compact distribution lines installed in parallel, with covered conductors, messenger wire, and spacers; (b) Covered conductor line with 15 kV rated voltage, Massachusetts, US; (c) Covered conductor line with 26.7 kV rated voltage, Canada (courtesy of Hendrix [5]).

Multiple three-phase lines with covered conductors may be installed in parallel at the same poles, either with the same rated voltage (see Fig. 1(a)) or underneath traditional overhead transmission lines at higher voltage level [4]. In the former configuration, the upmost messenger wires (MWs), whose position is established based on the desired insulation level, safety distance from ground (street level, buildings, etc.) defined by local regulations, and structural considerations, may intercept lightning and contribute in minimizing the incidence of direct strokes to the phase conductors; in other words, the MW may act as an "unintentional" shield wire, leading the current to ground at poles where it is connected to the grounding system. Furthermore, the MW may serve as a neutral conductor for grounded-wye systems, according to the distribution practice of some countries.

Several studies have investigated traveling voltages induced by indirect lightning [6], [7], or transients related to hybrid lines [8]. The aim of this paper is to investigate the

Project funded under the National Recovery and Resilience Plan (NRRP), Mission 4 Component 2 Investment 1.3 - Call for tender No. 1561 of 11.10.2022 of Ministero dell'Università e della Ricerca (MUR); funded by the European Union – NextGenerationEU (Project code PE0000021, Concession Decree No. 1561 of 11.10.2022 adopted by Ministero dell'Università e della Ricerca (MUR), CUP B53C22004070006, Project title "Network 4 Energy Sustainable Transition – NEST").

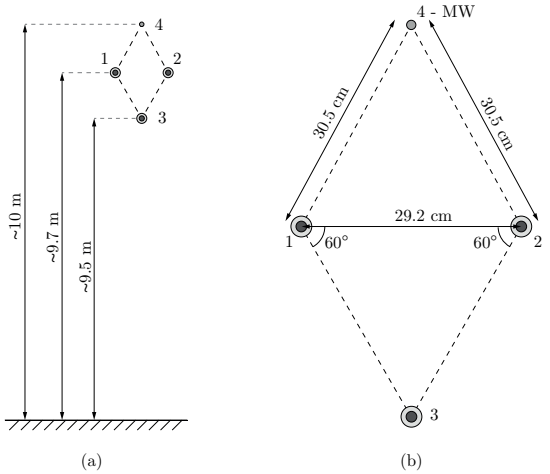

Fig. 2. Geometrical characteristics of the simulated aerial cable line. (a) Compact line above the ground. (b) Details of the arrangement of aerial cables and messenger wire.

characteristics of traveling voltage waves when the MW is hit by a direct lightning strike and grounded periodically. The purpose is to provide elements useful to consider the feasibility of employing covered conductors with the presence of the periodically grounded MW as a solution for improving the lightning performance of power overhead distribution lines.

The paper is organized as follows: Section II describes the distribution line under study and the modeling of its components; in Section III, the methodology adopted for the analysis is recalled, that is, the chain matrix analysis developed in the frequency domain for transmission lines characterized by a periodical structure; in Section IV voltages are analysed considering different grounding intervals and computing the effect of the distance between successive grounding points on the values of currents causing breakdown of the insulation. Conclusions and elements requiring further research are assessed in Section V.

II. Overhead Line Modeling

The chosen line configuration is displayed in Fig. 2. It consists of four conductors: three aerial cables (phases) and one bare conductor, that is, the messenger conductor. The phase conductors hang from the messenger by means of dielectric spacing devices (spacers), which also guarantee minimum variations in mutual distances between the aerial conductors along the span [2]. Installation guides of aerial cable systems suggest installing the spacers not only at the poles, but also along the span for mechanical support, at intervals approximately equal to 10 m.

The spacer and the covered conductors suitable for a medium voltage distribution line with rated voltage 20 kV were selected. The details of the system of conductors are found in Table 1. Operational practice requires the MW to be grounded at intervals shorter than 150 m through a grounding system offering a ground resistance r_{g} less then 30 Ω [9].

Table 1. Main modeling details of the aerial cable line.

Conductor	Phase	Phase	Phase	MW
Denomination	1	2	3	4
Conductor radius [mm]	7.11	7.11	7.11	6.15
Ins. thickness [mm]	6.74	6.74	6.74	-
Average height [m]	9.7	9.7	9.5	10.0
Resistance [mΩ/km]	194.5	194.5	194.5	590
Estimated BIL [kV]	513			
Reduction coefficient [7]	0.8			
DE (μs base)	56.25			
V_0 [kV]	347			

The matrix of per-unit-length (p.u.l.) inductances for the system of conductors in Fig. 2 was computed through standard transmission line analysis [10]; the elements of the matrix of p.u.l. capacitances were computed by means of the software Ansys 2D Extractor to account for the phase conductor insulation (with an assumed typical relative electric permittivity 2.25 for polyethylene).

It should be noted that volt-time curves for the line under study are not made available by the constructor, and that the impulse withstand voltage depends on the combined effect of the selected spacer (ensuring specific distances between the covered phase conductors and the MW) and the thickness and electrical properties of the insulating layer of the covered phase conductors. For the analyzed configuration, the Basic Insulation Level (BIL) is the only parameter estimated and made available by the constructor, relevant to assess the insulation withstand in a preliminary investigation. Following the common practice for overhead line insulation studies [11], the breakdown voltage is assumed to follow a Gaussian distribution with dispersion equal to 7%, leading to an estimated Critical Flashover Voltage $V_{\mathrm{CFO}} \approx 564$ kV.

However, since the BIL was evaluated as the algebraic sum of the BILs associated with the cable insulation and the air gap [12], a reduction coefficient equal to 0.8 is considered for the CFO of the system, in accordance with the indication in [7], raising from experimental tests on cable-insulator systems (i.e., combined-insulation systems similar to that considered). This CFO value (V_{CFO}, expressed in volt) is used to compute the parameters in (1), V_0 and DE, required for the application of the integration method to assess the insulation withstand to transient overvoltages [8], [11]:

$$V_0 = 0.77 \cdot V_{\mathrm{CFO}} \tag{1a}$$

$$\mathrm{DE} = 1.1506 \cdot V_{\mathrm{CFO}}^{1.36} \tag{1b}$$

The values of the used parameters are listed in Table 1. It should be recalled that these values were selected and computed based on some assumptions adopting an engineering approach, since only measurements of the impulse withstand voltage of the combined insulation (including the aerial cable insulation and the dielectric spacer for the line chosen arrangement and rated voltage) would allow the more accurate

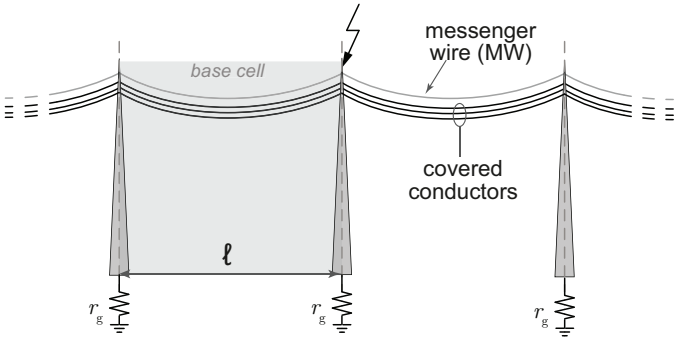

Fig. 3. Representation of the periodical structure of the aerial cable line under study, including the messenger wire, the covered phase conductors and periodical grounding at the poles with ground resistance r_g.

evaluation of the cumulative distribution function of the impulse breakdown voltages [4], [8].

III. Methodology of Analysis

The analysis is conducted by means of inverse Fourier transform of travelling voltages computed in the frequency domain by applying the chain matrix analysis for lines with periodical structure [13], [14]. The tool was first developed for typical overhead lines with bare conductors, but its application can be easily extended to study transverse electromagnetic propagation along any multiconductor transmission line, provided its periodicity and input of the necessary geometrical and electrical data. In the present study, this is ensured by the simulation of a uniform line with periodical grounding, that is, periodical connection of the MW to the line poles and grounding system, which are reasonably assumed to display unaltered geometric dimensions and electric properties along the line. Data regarding the p.u.l. capacitance and inductance matrix are passed as input.

With reference to the approach developed in [15], the propagation of traveling waves along the line span is described by the transmission matrix $[\mathbf{T_s}]$ (accounting for the span length ℓ); the transmission matrix $[\mathbf{T_g}]$ accounts for propagation along the half of the structure formed by the pole and the grounding system at its footing. Herein, a ground resistance $r_g = 30\,\Omega$ is considered. The base cell, which represents the main line section repeating periodically, consists of one line span, enclosed by two half-poles, shaded by the light grey area in Fig. 3. The total transmission matrix $[\mathbf{T}]$ of the base cell is computed consequently as follows:

$$[\mathbf{T}] = [\mathbf{T_g}]\,[\mathbf{T_s}]\,[\mathbf{T_g}] = \begin{bmatrix} [\mathbf{A}] & [\mathbf{B}] \\ [\mathbf{C}] & [\mathbf{D}] \end{bmatrix} \tag{2}$$

where the following matrices are introduced:

$$[\mathbf{T_g}] = \begin{bmatrix} [\mathbf{1}] & [\mathbf{0}] \\ [\mathbf{Y_g}] & [\mathbf{1}] \end{bmatrix} \tag{3}$$

$$[\mathbf{Y_g}] = \frac{1}{2}\begin{bmatrix} [\mathbf{0}] & [\mathbf{0}] \\ 0 & \mathrm{Y_{in}} \end{bmatrix} \tag{4}$$

In (2), $[\mathbf{A}], [\mathbf{B}], [\mathbf{C}], [\mathbf{D}]$ are submatrices of order 4, following the standard transmission matrix notation. In (3) and (4), $[\mathbf{1}]$ and $[\mathbf{0}]$, are the identity and the zero matrix, respectively; $[\mathbf{Y_g}]$ is a submatrix of order 4, accounting for half-a-pole; the pole is modeled as a lossless transmission line with characteristic resistance $R_t = 177\,\Omega$ [16] and propagation velocity equal to the speed of light in vacuum c_0. Indeed, expression (4) includes $\mathrm{Y_{in}}$, which represents the input admittance seen at the top of the pole, with ground resistance r_g.

The diagonalization of the submatrix $[\mathbf{A}]$ by means of the transformation matrix $[\mathbf{M}]$ produces a set of eigenvalues that allow for the computation of the set of propagation constants $\boldsymbol{\gamma}$ (at the right-hand side of (5), under the argument of the hyperbolic cosine function). Matrix $[\mathbf{M}]$, whose columns are the eigenvectors associated with those eigenvalues, is used in (6) to simply derive the matrix of characteristic admittances $[\mathbf{Y_w}]$ of the line with periodical grounding:

$$[\mathbf{M}]^{-1}\,[\mathbf{A}]\,[\mathbf{M}] = [\cosh(\boldsymbol{\gamma}\ell)] \tag{5}$$

$$[\mathbf{Y_w}] = [\mathbf{B}]^{-1}\,[\mathbf{M}]\,[\sinh(\boldsymbol{\gamma}\ell)]\,[\mathbf{M}]^{-1} \tag{6}$$

The novelty of the method consists in eliminating the need to describe backward and forward propagation through two different matrices of characteristic admittances; moreover, the matrix $[\mathbf{Y_w}]$ allows to implement the condition of matched line terminations accurately, avoiding to insert long line lateral sections with the only purpose of eliminating unwanted reflections from the terminations.

The frequency-domain voltages and currents at the input and output ports of the base cells of the periodical structure in Fig. 3 are computed using the transmission matrix $[\mathbf{T}]$ in (2) as:

$$\begin{bmatrix} [\mathbf{V_{in}}] \\ [\mathbf{I_{in}}] \end{bmatrix} = \begin{bmatrix} [\mathbf{A}] & [\mathbf{B}] \\ [\mathbf{C}] & [\mathbf{D}] \end{bmatrix} \begin{bmatrix} [\mathbf{V_{out}}] \\ [\mathbf{I_{out}}] \end{bmatrix} \tag{7}$$

where, in our case (longitudinally symmetric cells), the submatrices of $[\mathbf{T}]$ satisfy the following properties: $[\mathbf{A}] = [\mathbf{D}]^T$, $[\mathbf{B}] = [\mathbf{B}]^T$, and $[\mathbf{C}] = [\mathbf{C}]^T$, where superscript T stands for matrix transposition. The reader interested in the transmission matrix formalism and its application to multiport structures and multimodal propagation may, for instance, refer to [17] and [18].

IV. Simulation Results

Results aim at assessing the influence of the span length on the minimum current causing the insulation breakdown, with the modeling approach and assumptions presented in Section II. The CIGRE waveform is considered to simulate negative first stroke lightning currents [19], with channel impedance 200 Ω (the influence of the adopted channel impedance is investigated in [20]).

Two span lengths, $\ell = 50$ m and $\ell = 75$ m, are simulated. For each span length, simulations are conducted to account for the grounding of the MW at each pole (i.e., periodical grounding at distances equal to ℓ), or at alternate poles (i.e., periodical grounding at distances equal to 2ℓ). It should be noted that when the distance between successive grounding points is set to 150 m, results are valid also for describing

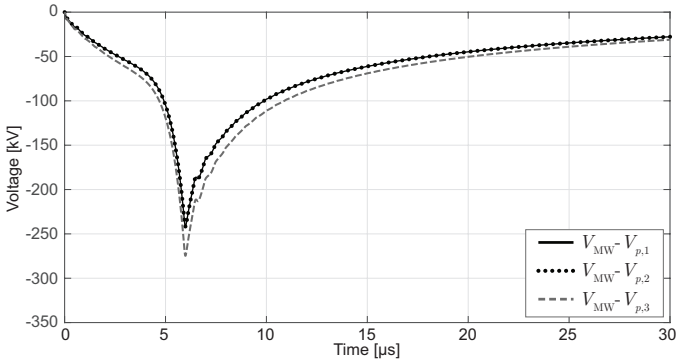

(a) Periodical grounding with 75 m interval.

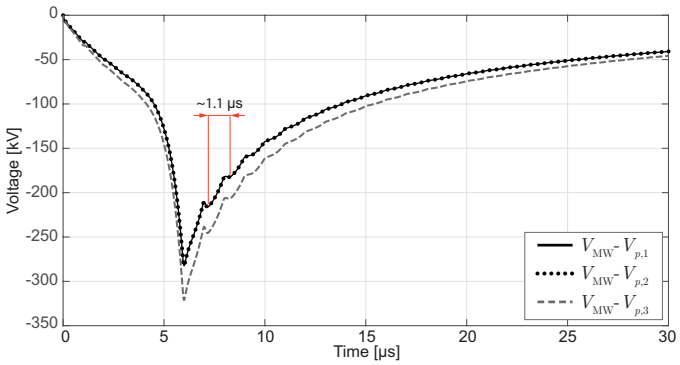

(b) Periodical grounding with 150 m interval.

Fig. 4. Voltage differences between the messenger wire (MW) and the covered phase conductors at the pole stricken by the lightning current with peak value 30 kA, not accounting for the normal operation voltages of the line with span length $\ell = 75$ m. Overvoltages with the messenger wire grounded periodically at distances (a) 75 m and (b) 150 m.

voltages along the line with $\ell = 50$ m, if the distance between two consecutive grounding points of the messenger is set to 3ℓ.

V_{MW} and $V_{\mathrm{p},k}$ denote the voltage-to-ground of the MW and of the k-th aerial cable (with $k = 1, 2, 3$), respectively; Figure 4 displays the voltages $(V_{\mathrm{MW}} - V_{\mathrm{p},k})$ computed for the case $\ell = 75$ m. Figure 4(a) refers to the configuration with the MW grounded at all poles, while Fig. 4(b) refers to the grounding of the MW at two-spans interval; for both grounding schemes, the lightning is assumed to strike a pole with grounded MW. Results are computed for a lightning current with peak value equal to 30 kA (median value for negative first stroke lightning currents [21]). No difference is found in the overvoltages associated with conductors 1 and 2, due to their symmetrical position with respect to the MW (as in Fig. 2).

A lower propagation velocity of travelling waves can be deduced from the period of reflections observed in Fig. 4 (e.g., $1.1\,\mu\mathrm{s} > 4\ell/c_0$ in Fig. 4(b)), as an expected consequence of the increased p.u.l. capacitances of the covered conductors, due to the outer insulation layer [22].

It is clear that grounding the MW at very short distances leads to the reduction of the overvoltage differences between the phase conductors and the MW. Performing the grounding of the MW at alternate poles, that is, doubling the distance

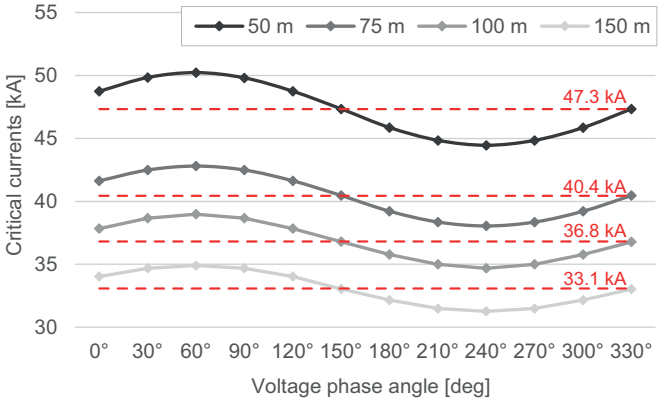

Fig. 5. Variation of the critical current peak value with the phase angle of the line operating voltage, different span lengths ($\ell = 50$ m, $\ell = 75$ m), and grounding intervals of the messenger wire (i.e., at all poles or at alternate poles). The lightning current is injected at the top of a pole where the messenger wire is grounded.

between subsequent grounding points, produces overvoltage peak values approximately equal to 1.16 p.u. with respect to those displayed in Fig. 4(a). In particular, reflected overvoltages, which are produced at the poles with grounded MW closest to the stricken pole where overvoltages are computed, travel back in times shorter than the time-to-peak of the impressed lightning overvoltage, affecting its rate of rise and peak value. When the MW is grounded at alternate poles, i.e., every 150 m, a smaller number of reflected waves travels back to the stricken pole, travelling longer distances, subject to bigger attenuation linked to the ground and conductor internal impedance.

Figure 5 shows the peak values of the critical currents causing insulation breakdown for different phase angles of the operating voltage (referring to conductor 1) and grounding distances, considering $\ell = 50$ m and $\ell = 75$ m as possible span lengths, and with the lightning striking a pole with grounded MW. The values of the critical current can be approximated by a sinusoidal function of the voltage phase angle; for each grounding scheme, the maximum deviation of the computed critical peak current with respect to the corresponding mean value is approximately 6%. Instead, grounding the MW at distances 2ℓ affects considerably the computed mean values of the critical currents, which are reduced to approximately 0.8 p.u. of the corresponding value computed when the MW is grounded at all poles.

Simulations are performed considering also the frequency response of the grounding system, which is assumed to consist of two vertical rods with radius 3 cm and length 1.2 m in order to get a low-frequency ground resistance $r_{\mathrm{g}} \simeq 30\,\Omega$. Values of the frequency-dependent ground impedance z_{g} are computed through the GEA simulator for different frequency values [23]. Due to the improved grounding performance of the two-rod system at high frequency, resulting essentially in a resistive-capacitive behavior of z_{g}, the computed critical currents are larger by approximately 1%.

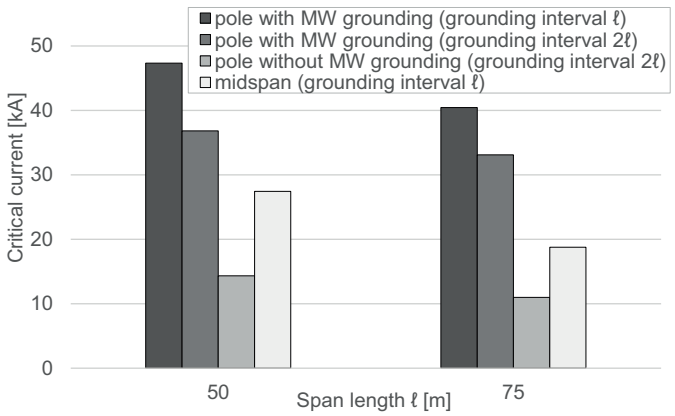

Fig. 6. Average critical current peak values computed for the line in Fig. 2 with span lengths $\ell = 50$ m and $\ell = 75$ m, grounding of the messenger wire at all poles or at alternate poles; the lightning current strikes the messenger wire in correspondence of a pole where it is or is not grounded, or at midspan.

Figure 6 compares the average value of the critical currents computed for the 12 operating voltage phase angles, simulating that the lightning current strikes the MW in correspondence of a pole where either it is grounded (considering grounding intervals ℓ and 2ℓ), or it is not connected to the pole grounding system (i.e., between two grounding points, considering the grounding interval 2ℓ). The average critical currents in the latter case are approximately 0.39 p.u. and 0.33 p.u. of the peak values computed with the lightning current being injected at a pole with grounded MW, with $\ell = 50$ m and $\ell = 75$ m, respectively, and grounding interval 2ℓ. This is caused by the larger impedance seen by the lightning current at the striking point, due to the lack of a direct connection of the MW to the pole grounding system.

Figure 6 also includes results for the direct lightning of the MW at midspan, and MW grounding at all poles. With both span lengths $\ell = 50$, 75 m, the computed average peak values of the critical current are bounded by those found with grounding interval 2ℓ. Current values associated with the direct lightning of the MW at a pole where it is not grounded represent the lower bound, due to the longer distance to be traveled by the voltage/current waves to reach a grounding point; instead, the upper bound is represented by current values computed with the lightning striking the MW at a grounding point, since a fraction of the injected current can be directly dispersed through the pole grounding system.

Lower average critical current peak values are found with $\ell = 75$ m, since the closest MW grounding points are located at further distance, i.e., 75 m $>$ 50 m, affecting the effectiveness of the MW grounding (associated with the physical mechanisms detailed previously).

It should be noted that a single set of parameters of the integral method is adopted to assess insulation withstand, referring to the expected BIL of the system. In this respect, since all critical current peak values were determined by the voltage difference $V_{\mathrm{MW}} - V_{\mathrm{p},3}$, the computed results are expected to be precautionary, due to the larger insulating distances and the position of the aerial cable 3 and the MW with respect to the dielectric spacer. Rigourously, different sets of parameters linked to the different phase aerial cables should be used to asses the occurrence of phase-to-MW insulation breakdown.

V. Conclusion

The paper presents an analysis of a compact distribution line with covered phase conductors and a messenger wire. The advantages of applying a methodology based on the chain matrix approach are described, showing that the definition of a single matrix of characteristic admittances is convenient for the analysis of lines with periodical grounding.

The grounding scheme and the chosen span length have been shown to hold predominant effect, compared to the operating voltage phase angle, on the computed critical current peak values for which the impulse withstand of the line insulation is not guaranteed. As to the computation of the actual peak value of the critical currents, a more accurate analysis should firstly exploit the cumulative distribution function of the impulse breakdown voltages obtained from measured data for the line configuration under study.

Acknowledgment

The authors would like to thank Dr. B. J. Trager from Marmon Utility for sharing his expertise and providing valuable insight to the conducted research.

References

[1] *IEEE Guide for Electric Power Distribution Reliability Indices*, IEEE Std. 1366, Sep. 2022.

[2] R. Powell, H. Thwaites, and R. Stys, "Estimating lightning performance of spacer-cable systems," *IEEE Transactions on Power Apparatus and Systems*, vol. 84, no. 4, pp. 315–319, 1965.

[3] G. S. Lima, R. M. Gomes, E. Ronaldo Filho, A. De Conti, F. H. Silveira, S. Visacro, and W. A. Souza, "Influence of XLPE-covered cables on the impulse withstand voltage of a single-phase structure used in compact distribution lines," in *2015 International Symposium on Lightning Protection (XIII SIPDA)*. IEEE, 2015, pp. 260–263.

[4] A. Borghetti, G. Ferraz, F. Napolitano, C. Nucci, A. Piantini, and F. Tossani, "Lightning protection of a compact MV power line sharing the same poles of a HV line," in *2018 34th International Conference on Lightning Protection (ICLP)*. IEEE, 2018, pp. 1–7.

[5] "Spacer cable vs. tree wire: Pros and cons of two distinct construction options," https://www.powerandcables.com/wp-content/uploads/2017/04/Spacer-Cable-v-Tree-Wire-Pros-Cons-Of-Aerial-Cable-Systems-1.pdf, accessed: 2024-02-20.

[6] A. De Conti, A. C. Silva, and O. E. Leal, "Transient analysis of compact distribution lines with dielectric-coated phase cables," *Electric Power Systems Research*, vol. 181, p. 106173, 2020.

[7] S. Yokoyama, T. Sato, S. Shozo, and Y. Hashimoto, "Lightning performance of insulated wires on overhead power distribution lines," in *2010 30th International Conference on Lightning Protection (ICLP)*. IEEE, 2010, pp. 1–4.

[8] L. B. Moraes, A. Piantini, and M. Shigihara, "Insulator models of a hybrid overhead line," in *2023 International Symposium on Lightning Protection (XVII SIPDA)*. IEEE, 2023, pp. 1–6.

[9] *Hendrix Covered Conductor Manual*, Western Power, 2013.

[10] C. R. Paul, *Analysis of Multiconductor Transmission Lines*. John Wiley and Sons, 2008.

[11] A. R. Hileman, *Insulation Coordination for Power Systems*, C. Press, Ed. CRC Press, 1999.

[12] "Spacer cable lightning performance," https://www.tdworld.com/overhead-distribution/article/21276547/spacer-cable-lightning-performance, accessed: 2024-02-20.

[13] E. Stracqualursi, R. Araneo, J. A. Brandão Faria, and A. Andreotti, "Application of the transfer matrix approach to direct lightning studies of overhead power lines with underbuilt shield wires Part I: Theory," *IEEE Trans. Power Del.*, vol. 37, no. 2, pp. 1226–1233, 2022.

[14] ——, "Application of the transfer matrix approach to direct lightning studies of overhead power lines with underbuilt shield wires part II: Simulation results," *IEEE Trans. Power Del.*, vol. 37, no. 2, pp. 1234–1241, 2022.

[15] ——, "Protection of distribution overhead power lines against direct lightning strokes by means of underbuilt ground wires," *Electric Power Systems Research*, vol. 202, p. 107571, 2022.

[16] M. H. T. Hara, O. Yamamoto and C. Uenosono, "Empirical formulas for surge impedance for single and multiple vertical conductors," *IEEJ Trans. Power Energy*, vol. B-110, pp. 129–136, 1990.

[17] J. A. Brandão Faria, "The transfer matrix method: Analysis of nonuniform multiport systems," *IEEE Access*, vol. 8, pp. 23 650–23 662, Feb. 2020.

[18] ——, "Multimodal propagation in multiconductor transmission lines," *Journal of Electromagnetic Waves and Applications*, vol. 28, no. 14, pp. 1677–1702, 2014.

[19] "Guide to procedures for estimating the lightning performance of transmission lines," *CIGRE Technical Brochure*, vol. 63, 1991.

[20] Z. G. Datsios, P. N. Mikropoulos, and T. E. Tsovilis, "Effects of lightning channel equivalent impedance on lightning performance of overhead transmission lines," *IEEE Trans. Electromagn. Compat.*, vol. 61, no. 3, pp. 623–630, 2019.

[21] C. a. WG C4.407, *Lightning Parameters for Engineering Applications*. Cigré TB549, Aug. 2013.

[22] A. C. Silva, A. De Conti, and Ó. E. Leal, "Lightning wave propagation characteristics of an overhead line with insulated phase conductors," in *2018 34th International Conference on Lightning Protection (ICLP)*. IEEE, 2018, pp. 1–6.

[23] E. Stracqualursi and R. Araneo, "Grounding Electromagnetic Analysis (GEA) simulator," https://sites.google.com/view/geasimulator/home-page?authuser=4, 2024.